Bulletin of Mathematical Biology (2022) 84:127
https://doi.org/10.1007/s11538-022-01076-6

Society for Mathematical Biology

ORIGINAL ARTICLE

Discrete Models in Epidemiology: New Contagion Probability Functions Based on Real Data Behavior

Alexandra Catano-Lopez[1] · Daniel Rojas-Diaz[1] · Diana Paola Lizarralde-Bejarano[1] · María Eugenia Puerta Yepes[1]

Received: 23 March 2022 / Accepted: 29 August 2022 / Published online: 22 September 2022

Abstract

Mathematical modeling is a tool used for understanding diseases dynamics. The discrete-time model is an especial case in modeling that satisfactorily describes the epidemiological dynamics because of the discrete nature of the real data. However, discrete models reduce their descriptive and fitting potential because of assuming a homogeneous population. Thus, in this paper, we proposed contagion probability functions according to two infection paradigms that consider factors associated with transmission dynamics. For example, we introduced probabilities of establishing an infectious interaction, the number of contacts with infectious and the level of connectivity or social distance within populations. Through the probabilities design, we overcame the homogeneity assumption. Also, we evaluated the proposed probabilities through their introduction into discrete-time models for two diseases and different study zones with real data, COVID-19 for Germany and South Korea, and dengue for Colombia. Also, we described the oscillatory dynamics for the last one using the contagion probabilities alongside parameters with a biological sense. Finally, we highlight the implementation of the proposed probabilities would improve the simulation of the public policy effect of control strategies over an infectious disease outbreak.

Daniel Rojas-Diaz, Diana Paola Lizarralde-Bejarano and Maria Eugenia Puerta Yepes have contributed equally to this work.

✉ Alexandra Catano-Lopez
acatano@eafit.edu.co

Daniel Rojas-Diaz
drojasd@eafit.edu.co

Diana Paola Lizarralde-Bejarano
dlizarra@eafit.edu.co

María Eugenia Puerta Yepes
mpuerta@eafit.edu.co

[1] School of Applied Sciences and Engineering, Universidad EAFIT, Medellín, Antioquia, Colombia

Keywords Discrete · Compartmental models · Contagion probability · Heterogeneous population

1 Introduction

Using discrete mathematical models for the study of disease transmission has increased because of the expansion of the diseases, health entities collect the data in discrete-time units, making it a natural option to describe the transmission of diseases (Cao and Tan 2015). The discrete models show a richer dynamical behavior than continuous models, getting more diverse results for long-term diseases (Cao and Tan 2015; Li and Li 2018). This advantage could be more appropriate for vector-borne diseases, where time scales for the dynamics of the human and mosquito populations are significantly different (Li and Li 2018).

However, some models assume that diseases spread over a homogeneous population (Anastassopoulou et al. 2020). This assumption is linked to the definition or paradigm of the contagion probabilities for each model. Thus, the way to design some expressions, as the probabilities of contagion, affects the analysis of the spread of the disease in large-scale populations and studies (Catano-Lopez and Rojas-Diaz 2020), e.g., the classical expression of susceptible per infection over total population commonly used in continuous and discrete models (Wonham et al. 2004; Li and Li 2018). Its expression does not include variations that a population might suffer due to human behavior as the distance between individuals (Cabrera et al. 2021) or the heterogeneous mixing between humans and vectors (Kong et al. 2018), among others.

Some other authors have proposed different ways of approaching to handle the homogeneity problem, for continuous and discrete models. Cabrera et al. (2021) present a transmission rate that depends on the social distance for transmission of respiratory infectious diseases; Kong et al. (2018) describe transmission function based on a negative binomial distribution to characterize the heterogeneity in infectious interactions of humans and mosquitoes. Sabatier et al. (2004) present a series of multiple discrete probabilities similar as the structure described by Martcheva (2015) for discrete-time models related to sheep flock diseases. Sometimes these contagion expressions become complex, not very intuitive, or practical approaches for public policies development. Thus, we develop contagion probability functions that meet the propagation principles in networks during the modeling process, which preserve a biological sense and handle to fit models to real data of different localities as Germany and South Korea (for COVID-19) and Colombia (for dengue).

We divide the paper as follows: a method section that describes the fundamental properties of contagion probabilities wide proposed in the literature (Castillo-Chavez and Yakubu 2001; Martcheva 2015), the structure of discrete compartmental models and the data implemented to fit them. Then, we express the construction of the probabilities functions with heterogeneity expression alongside the numerical experiments implementing data of COVID-19 and dengue from different localities. Finally, we present the discussion and conclusions of implementing the new probability functions on two diseases.

2 Methodology

2.1 Case Studies: COVID-19 and Dengue Diseases

Health systems quantify the effect of the disease in affected populations because epidemics have explosive characteristics that depend on the nature of the diseases and involve the type of transmission. Thus, we address in this study two different diseases according to their contagion sources, e.g., human–human and human–vector diseases as COVID-19 and dengue, respectively.

COVID-19 it is a direct-transmitted infectious disease caused by the SARS-CoV-2 virus with main symptoms related to respiratory illness (Fink et al. 2020). It became a worldwide issue because of its high transmission rate, even affecting social behaviors, where processes such as quarantine and lockdowns became a daily dynamic in human populations. COVID-19 affected countries with a high population density, low control policies and limited health systems; it generates multiple and consecutive outbreaks or behaviors different from the classical bell-form of reported cases. For example, Germany presented one peak and oscillations in reported cases; also, South Korea presented two consecutive outbreaks. For that reason, we took these countries to model and fit the COVID-19 dynamics. We use the data of the number of active (total—recovered—dead cases) reported from March 3, 2020, to September 19, 2020, for Germany and February 2, 2020, to September 27, 2020, for South Korea (Dong et al. 2020).

Dengue behind COVID-19, other endemic diseases in vulnerable regions are considered a public health issue, e.g., dengue virus as the vector-borne disease transmitted by *Aedes* females in some tropical and subtropical regions as Colombia. Thus, we chose the municipalities of Bello and Itagüí, located in Aburrá Valley (Antioquia, Colombia), as study sites. Bello and Itagüí are overcrowded localities with a population of 407,000 and 207,000 inhabitants in 2010 (DANE 2011). These regions have endemic dengue transmission and have shown co-circulation of the four dengue serotypes over the last ten years (Usme-Ciro et al. 2008; Vega 2013; Peña-García et al. 2016). Also, they presented two dengue outbreaks: (i) Bello from the 49th epidemiological week in 2009 to the 34th epidemiological week in 2011 and (ii) Itagüí from the 9th epidemiological week in 2010 to the 2nd epidemiological week in 2011. The data are a time series of the new cases of dengue per week reported in the Public Health System (SIVIGILA by its Spanish initials).

Note that COVID-19 and dengue cases have different sampling times because of their natural history and the resources invested for their identification. The health systems weekly report dengue in Colombia, while COVID-19 is daily in some countries such as Germany and South Korea. Thus, the way we sample the phenomena would involve modeling the real system.

2.2 Basic Structure for Discrete Compartmental Models

The explosive characteristics and emergence of new outbreaks are a cause of studying diseases using mathematical models, even for new diseases (COVID-19) and endemic ones (dengue). There are different ways to represent and study the transmission phenomenon, e.g., mathematical models as discrete compartments. Several authors give basic structures to define the model structure; in this paper, we follow the structure introduced by Martcheva (2015) and Allen (1994) to create models for the transmission of COVID-19 and dengue because they are diseases that need two different compartment representation.

We based on a classic representation of a SIRS for human-to-human direct transmission, with a constant population of N and a mortality probability μ, allowing a periodic behavior of the disease (Allen 1994); with this basic structure, we present two new discrete models in Sect. 3.2: one for COVID-19 and another one for vector-borne diseases as dengue.

For COVID-19, we disaggregate the susceptible S, infected I and recovered R compartments into free circulation (S_f and I_f), quarantined (S_q and I_q), and identified individuals (I_j) as some authors suggested for direct diseases as SARS (Zhou et al. 2004). For the vector-borne case, as classically shown in the literature, we create a compartmental system for each population, i.e., a SIR model for humans and a SI model for the vector in which we connect both models by an expression that represents a contagion probability, $G(\cdot)$. There are different ways to define this probability (see Table 4 in "Appendix A"), inclusive some authors set it is as a modeling issue or paradigm (Cabrera et al. 2021).

2.3 Definition of Contagion Probabilities for Discrete Models

The way to represent the contagion contacts in a discrete-time model depends on the definition of the prevalence function $G(I/N)$ in time t. This function determines the fraction of the susceptible population becoming infected for the next time step. For this work, we will follow the guidelines proposed in Castillo-Chavez and Yakubu (2001), that requires such function to satisfy the following conditions:

1. $G : [0, \infty) \to [0, 1]$
2. $G(0) = 0$
3. G is a monotone increasing function with $G'(x) \geq 0$ and $G''(x) < 0$.

The first condition delimits the range of the function to the range of a probability. The second one indicates that the chance of developing a disease is zero when there are no infected individuals in the population. The third condition specifies that the contagion expression increase as the number of infected increases. The last property could be modified according to the population behavior against the disease; because as in the COVID-19 case, not all diseases obey its classical representation because of factors such as the heterogeneity of the population, the connections inside the population or the control of health entities. Thus, we proposed different functions for the contagion probability according to the execution of the human interaction with the

infectious resource (human or vector depending on the addressed disease). Also, we introduce the concept of heterogeneity to these proposed expressions.

2.4 Numerical Approach: Fitting Discrete Models with Real Data

We exemplify the uses of the new proposed probabilities using them in discrete-time models that present different paradigms of infection: COVID-19 and dengue outbreaks. We fit the COVID-19 model to detected active cases using the state I_j (see Eq. (6) in Results 3.2.1). Otherwise, we fit the dengue model with an output that represents instantaneous cases per week (see Eq. (10) in Results 3.2.2).

For the COVID-19 case, we test and compare the different probabilities with each other because all probabilities fit the direct human transmission. Otherwise, for the dengue case, we do not compare probabilities because the paradigm of human–vector transmission is represented by the fusion of the probabilities. We performed all numerical experiments using MATLAB 2020a and the GSUA_CSB toolbox (Rojas-Díaz and Vélez-Sánchez 2019), in which we estimated parameters using the Interior-Point Algorithm with Analytic Hessian in GSUA_CSB toolbox; those experiments and their results are available in GitHub https://github.com/alexacl95/ContagionProbability repository for each locality.

3 Results

We present two main results related to the definition and implementation of the contagion probabilities. First, we define their mathematical structure according to the individual election and add an expression to represent the heterogeneity of populations during the contagion dynamics. Then, we implement in two models the contagion probabilities following two paradigms: direct transmission diseases as COVID-19 and vector-borne diseases as dengue.

3.1 Formulation of Probabilities of Contagion and Their Properties

It is common in the literature to find definitions for $G(\cdot)$ that describe the spread of infectious diseases through contact between susceptible and infectious individuals (Chávez et al. 2017; Fink et al. 2020), especially discrete expressions derived from expressions as e^{-x} or $x(x+1)^{-1}$ (Hernandez-Ceron et al. 2013; Martcheva 2015) (see Table 4 in "Appendix A"). Thus, we propose new functions for contagion probability based on the idea of consuming the networks through disease expansion within a heterogeneous population. For notation summarization, we define all time-dependent states without (t) through the explanations document where appropriate, e.g., the population states.

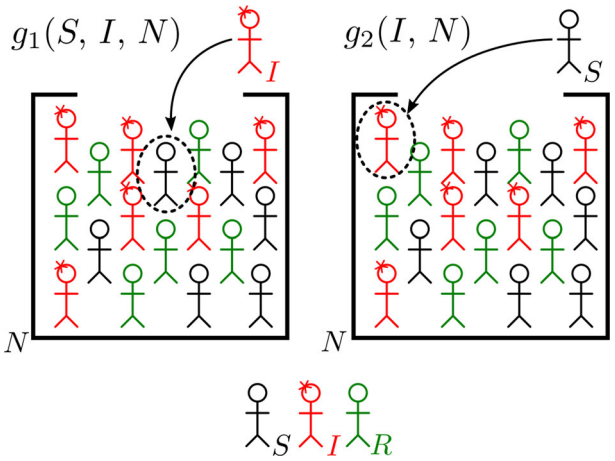

Fig. 1 We exemplify the contagion functions through the dynamic of individual selection. The main idea is similar to the analogy of selecting a ball of a specific color in a bag full of balls: let be the total population in a bag full of people in different states (S, I and R). The probability of an I to choose an S individual over the whole population is g_1 and vice versa is g_2 (color figure online)

3.1.1 Probability of Contagion from Interaction with Living Carriers

First, assume we have a homogeneous population of susceptible $S \geq 1$ and $I \geq 0$ the number of disease carriers. Then, the number of *infectious interactions* that reach S would be zIS/N, where z is the mean number of interactions that a member of the population exerts over another one. If we consider that interaction as a process of choice, we could define two contagion paradigms described as probability functions g_1 and g_2 (see Fig. 1):

1. $g_1(S,\ I,\ N)$ is the probability of S to receive an infectious interaction from an infected individual I; i.e., an S is chosen at least once.

$$g_1(S,\ I,\ N) = 1 - \left[1 - \tfrac{1}{S}\right]^{zI\frac{S}{N}} \tag{1}$$

   Note that an infected individual could be composed of individuals from another species population, e.g., a vector species as mosquitoes (see Sect. 3.2.2, for the dengue study case).

2. $g_2(I,\ N)$ is the probability of a S establishing interaction with an I at least once, i.e., an S choose an I.

$$g_2(I,\ N) = 1 - \left[1 - \tfrac{I}{N}\right]^{z} \tag{2}$$

   Now, note that we assume the total population N is homogeneous for the basic definition. However, in Sect. 3.1.2 we propose an expression to overcome it.

The occurrence probability of one infectious interaction that involves a susceptible individual must be defined as

$$G_T(S,\ I,\ N) = g_1(S,\ I,\ N) + (1 - g_1(S,\ I,\ N))g_2(I,\ N)$$

Now, a natural way for defining $G(\cdot)$ is

$$G(S,\ I,\ N) = \beta\, G_T(S,\ I,\ N)$$

where β is the probability of a S getting infected after at least one infectious interaction. It is possible to define the function $G(S,\ I,\ N)$ through $g_1(S,\ I,\ N)$ or $g_2(I,\ N)$, separately. That election should respond to the interest of the researchers and the nature of the disease under study. For instance, $g_1(S,\ I,\ N)$ is appropriate to model vector-borne diseases, while $g_2(I,\ N)$ is not because hosts do not choose vectors; we can see this in Sect. 3.2.2 during the model description. Finally, in "Appendix B" we present the proofs that the proposed probabilities meet the conditions described in Sect. 2.3.

3.1.2 Overcoming the Homogeneous Population Issue

In the above subsection, we defined the probabilities under the assumption of a homogeneous population (see Fig. 1). However, it is a debated assumption in the literature (Anastassopoulou et al. 2020). To overcome the homogeneity assumption, we added a mathematical expression to the proposed probabilities g_1 and g_2 that approach it by redefining the total population as an incomplete graph (see Fig. 2).

If we represent the total population over a spatial area as a graph whose nodes are individuals, it becomes equivalent to a complete graph under the homogeneity assumption. For an epidemiological model, the homogeneous population produces a bell-shaped output for actively infected individuals, not a feasible behavior for multiple outbreaks. We took the idea of the graph and rebuilt it as many strongly connected subgraphs (clusters) and a few edges connecting one cluster to another. At the start of the outbreak, the rapid dispersion of the disease gradually slows down, followed by oscillations or plateau-shaped behavior in the infected cases; this is an effect of consuming the contagion networks within each cluster.

It should be possible to induce this behavior in discrete-time models by defining a function of S and I in a way such that the number of infectious contacts decreases whether I increases or S decreases. Since the probabilities we defined in previous sections involves proportions, a natural way to define that function is

$$\aleph(S, I) = 1 + \nu\, \frac{I}{S+I}$$

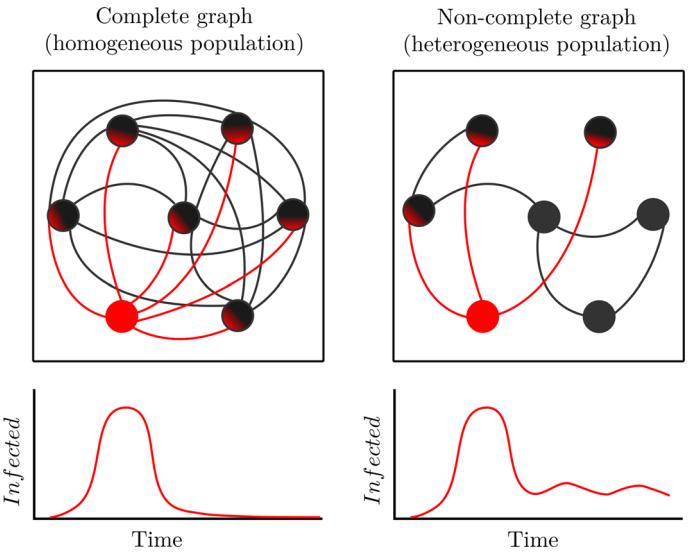

Fig. 2 Graph representation of the contact in a population. The left side represents a homogeneous population: if we introduce an infected individual I, it has the same probability to interact with any individual of the population, creating a bell-shaped output. The left side represents a heterogeneous population: if we introduce an infected individual I, it does not have direct contact with the total population at the time, implying a delay in the disease's spread because of the different contagion networks, creating a plateau or oscillatory infective output (color figure online)

where ν is the parameter of intrinsic isolation and then implement it in (1), and (2) to decrease probability of contact whenever I increases or S decreases. Hence, contact probabilities are redefined as follows

$$G_1(S,\ I,\ N) = 1 - \left[1 - \tfrac{1}{S}\right]^{zI\left(\frac{S}{N}\right)^{\aleph(S,\ I)}} \tag{3}$$

$$G_2(S,\ I,\ N) = 1 - \left[1 - \left[\tfrac{I}{N}\right]^{\aleph(S,\ I)}\right]^{z} \tag{4}$$

Also, $\aleph(S,\ I)$ expression can be implemented in other probability functions, as the classical one:

$$G_3(S,\ I,\ N) = (I/N)^{\aleph(S,\ I)} \tag{5}$$

Although the (5) has a connectivity expression, it does not represent the same behavior as (3) and (4) and does not take into account a parameter for the number of infectious interactions.

Note that with the $\aleph(S,\ I)$ expression, the modified probabilities meet the first and second properties described in Sect. 2.3. Even so, they do not necessarily meet the third one, giving diverse behaviors in the probability that match with some burnout

of the infection network in diseases such as COVID-19 because they are related to human behavior, especially to the distance between individuals.

3.1.3 Numerical Approach for Contagion Probabilities

We present how the change in parameters could affect the contagion probabilities behavior. First, using the derivatives we have

$$\frac{\partial G_2(S,I,N)}{\partial \nu} < 0 \quad \frac{\partial G_1(S,I,N)}{\partial \nu} < 0$$
$$\frac{\partial G_2(S,I,N)}{\partial z} > 0 \quad \frac{\partial G_1(S,I,N)}{\partial z} > 0$$

where the probabilities decrease by increasing the connection parameter (ν), i.e., the population acquires a heterogeneous behavior. On the other hand, the infectious probabilities increase by varying z, representing the mean number of infectious contacts. Also, we identified that $G_2(S,\ I,\ N)$ and $G_1(S,\ I,\ N)$ are concave down for z

$$\frac{\partial^2 G_1(S,I,N)}{\partial z^2} < 0 \quad \frac{\partial^2 G_2(S,I,N)}{\partial z^2} < 0$$

and concave up and down for ν meeting the following conditions:

$$\frac{\partial^2 G_1(S,I,N)}{\partial \nu^2} > 0 \text{ for } z > \frac{-1}{I\log(1-1/S)(S/N)^{-\aleph(S,I)}}$$
$$\frac{\partial^2 G_1(S,I,N)}{\partial \nu^2} < 0 \text{ for } z < \frac{-1}{I\log(1-1/S)(S/N)^{-\aleph(S,I)}}$$

$$\frac{\partial^2 G_2(S,I,N)}{\partial \nu^2} > 0 \text{ for } z < (I/N)^{-\aleph(S,I)}$$
$$\frac{\partial^2 G_2(S,I,N)}{\partial \nu^2} < 0 \text{ for } z > (I/N)^{-\aleph(S,I)}$$

These mathematical properties allow a rich behavior for probabilities values in an epidemic, in which the heterogeneity could increase for the different conditions of the infected population increase or decrease.

In Fig. 3, we present a numerical example using smoothed data from South Korea (see Sect. 2.1 for data methodology). This figure illustrates different function behaviors by varying parameters z and ν. For z, we identify a vertical displacement of the solution; for ν, we can see a deformation of the original form of the function.

3.2 Numerical Results: Implementation of Contagion Probabilities in Compartmental Models

We present two model paradigms, one for direct transmission diseases as COVID-19 and the other for vector-borne diseases. For both cases, we describe the mathematical model, the fitting process and the parameter values estimated for each locality.

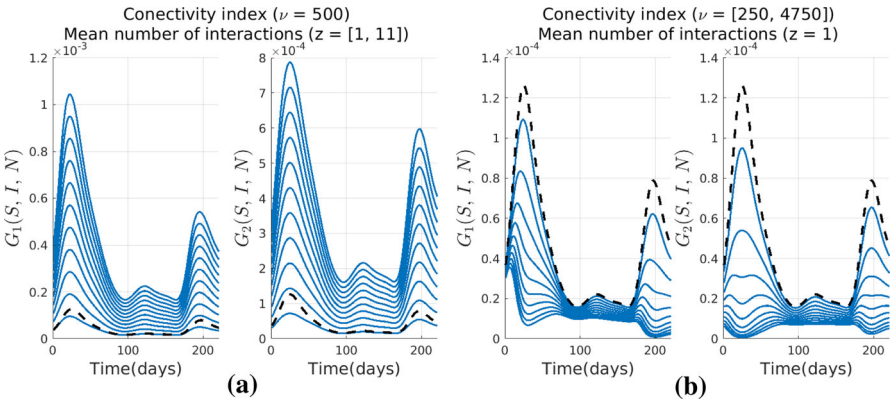

Fig. 3 Monte Carlo simulations using Eqs. (3) and (4). The black dotted lines represent the functions $G_2(S,\ I,\ N)$ and $G_1(S,\ I,\ N)$) evaluated with the real data (number of active cases in Korea), $z = 1$ and $\nu = 0$. In a) the blue lines are $G_2(S,\ I,\ N)$ and $G_1(S,\ I,\ N)$ simulations with $\nu = 500$ and varying z in the interval $[1,\ 11]$. In b) the blue lines are $G_2(S,\ I,\ N)$ and $G_1(S,\ I,\ N)$ simulations with $z = 1$ and ν in the interval $[250,\ 4750]$ (color figure online)

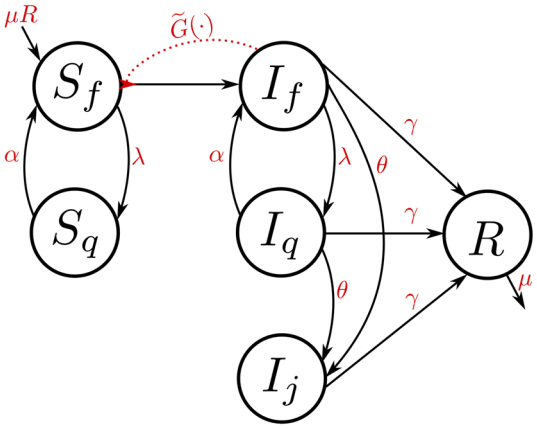

Fig. 4 Representation of a SIRS model by desegregating susceptible population into S_f and S_q, and infected population I_f, I_q and I_j (color figure online)

3.2.1 Direct Transmission Diseases: COVID-19 Case

In Eq. (6) and Fig. 4, we present a discrete model with quarantines and identification compartments for direct transmission diseases as COVID-19. First, we defined the population flows between compartments: the susceptible population in free circulation could become infected with a probability $\beta\widetilde{G}(\cdot)$ (see Eq. (7)). Also, they could enter quarantine with probability λ and leave it with probability α. The infected population could be in free circulation α, quarantine λ, or be detected and completely isolated θ. Infected individuals recovered from the disease with a probability γ and could lose

immunity with a probability μ (for more information and descriptions see Table 1).

$$\begin{aligned} S_f(t+1) &= S_f(1-\beta\widetilde{G}(\cdot))(1-\lambda) + S_q(t)\alpha + \mu R(t) \\ S_q(t+1) &= S_f(t)(1-\beta\widetilde{G}(\cdot))\lambda + S_q(t)(1-\alpha) \\ I_f(t+1) &= S_f(t)\beta\widetilde{G}(\cdot) + I_f(t)(1-\gamma)(1-\theta)(1-\lambda) \\ &\quad + I_q(t)(1-\gamma)(1-\theta)\alpha \\ I_q(t+1) &= I_f(t)(1-\gamma)(1-\theta)\lambda + I_q(t)(1-\gamma)(1-\theta)(1-\alpha) \\ I_j(t+1) &= (I_f(t)+I_q(t))(1-\gamma)\theta + I_j(t)(1-\gamma) \\ R(t+1) &= R(t)(1-\mu) + \gamma(I_f(t)+I_q(t)+I_j(t)) \end{aligned} \tag{6}$$

For the contagion probabilities $\widetilde{G}(\cdot)$ in Eq. (6), we implemented the proposed functions $\widetilde{G}_1$ and $\widetilde{G}_2$ based on Eqs. (3) and (4):

$$\begin{aligned} \widetilde{G}_1(S_f,\ I_f,\ N) &= 1 - \left(1 - \tfrac{1}{S_f}\right)^{zI_f(S_f/N)^{\aleph(S_f,I_f)}} \\ \widetilde{G}_2(S_f,\ I_f,\ N) &= 1 - \left(1 - \left[\tfrac{I_f}{N}\right]^{\aleph(S_f,I_f)}\right)^{z} \end{aligned} \tag{7}$$

with $\aleph(S_f, I_f) = 1 + \nu\frac{I_f}{I_f+S_f}$ and $I_T = I_f + I_q + I_j$ the infected population. Note that, because of the quarantines in the model, the contagion equations focused on free circulation susceptible and infectious populations.

The probabilities implementation depends on the modeler's interest to represent the infection dynamics. Thus, we add to the performance analysis the classical contagion probability

$$\widetilde{g}_3(I_f) = I_f/N \tag{8}$$

and the classical one by adding the heterogeneity expression $\aleph$

$$\widetilde{G}_3(S_f,\ I_f,\ N) = (I_f/N)^{\aleph(S_f,I_f)}$$

We performed 2000 parameter estimations for Germany and South Korea using the basic structure in (6) with the different proposed probabilities ($\widetilde{G}_2$ and $\widetilde{G}_1$) and the modified ones ($\widetilde{G}_3$ and $\widetilde{g}_3$). We selected the best parameter estimations by its cost function value and visual fitting. Figure 5 presents the multiple fits for each locality according to the mentioned functions. The models with $\aleph$ expression ($\widetilde{G}_2$, $\widetilde{G}_1$ and $\widetilde{G}_3$) present notorious oscillations, better fitting the model with $\widetilde{G}_1$ since the model with $\widetilde{g}_3$ could not follow the oscillations for no locality.

We present the parameter values for the best fits for all functions and both localities in Table 2. The values for quarantine-related parameters (λ and α) indicate that the population did not leave or enter often to quarantine for model structures with $\aleph$ expression; thus, $\widetilde{g}_3$ indicates the highest probability of leaving the quarantine. For models with new infection probabilities ($\widetilde{G}_2$ and $\widetilde{G}_1$), the θ values indicate that both

Table 1 Parameter and states (factors) definition for both models

Factors	Definition	Estimation range
$S_f(0)$	Free-circulation susceptible population	–
$S_q(0)$	Quarantined population	–
$I_f(0)$	Free-circulation infected population	–
$I_q(0)$	Quarantined infected population	–
$I_j(0)$	Identified infected population	–
$R(0)$	Non-identified recovered population	–
$R_j(0)$	Identified recovered population	–
N	Total human population	
λ	Probability of entering quarantine	[0, 1]
α	Probability of leaving quarantine	[0, 1]
μ	Probability of mortality/immunity lost	[0, 0.01]
θ	Identification probability	[0, 1]
γ	Human recovery probability	[0, 1]
ν	Connectivity index	[0, 1000]
z	Number of direct infective interactions	[0, 30]
β	Infection probability	[0, 1]

We present the range for each factor as the values that can take in initial conditions (states) and alongside its dynamics (parameters and functions)

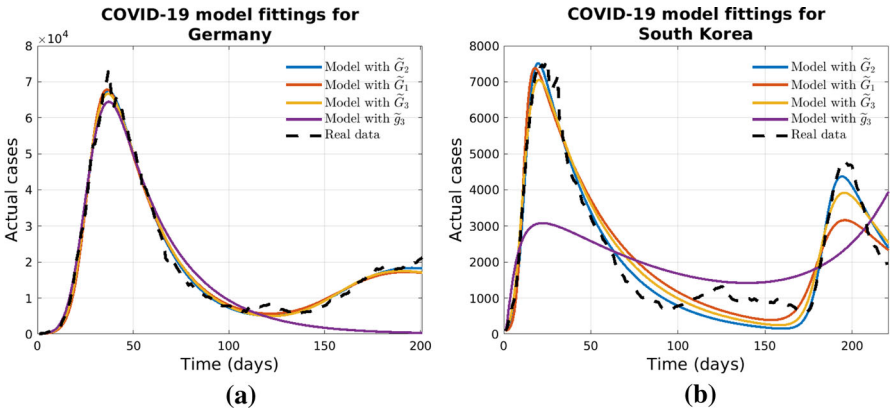

Fig. 5 Discrete model (6) fitted to real data for a) Germany and b) South Korea with the probabilities given by Eqs. (7) and (8); we present the parameters in Table 2. The cost functions for Germany fittings are $2.0751e^6$, $2.0766e^6$, $2.0765e^6$ and $2.151e^6$ for $\widetilde{G}_2$, $\widetilde{G}_1$, $\widetilde{G}_3$ and $\widetilde{g}_3$, respectively; and the cost functions for South Korea are $1.50e^5$, $1.511e^5$, $1.497e^5$ and $1.43e^5$ for $\widetilde{G}_2$, $\widetilde{G}_1$, $\widetilde{G}_3$ and $\widetilde{g}_3$ (color figure online)

localities presented a high identification of infected individuals. Then, in the case of $\aleph$, Germany is a less connected place than South Korea because the ν value is fewer for the first than for the second one.

Table 2 Estimated parameters for outbreaks occurred in Germany and South Korea using the discrete model in (6) with each contagion probability ($\widetilde{G}_2$, $\widetilde{G}_1$, $\widetilde{G}_3$ and $\widetilde{g}_3$)

Factors	Germany				Korea			
	$\widetilde{G}_1$	$\widetilde{G}_2$	$\widetilde{G}_3$	$\widetilde{g}_3$	$\widetilde{G}_1$	$\widetilde{G}_2$	$\widetilde{G}_3$	$\widetilde{g}_3$
$S_f(0)$	$8.3e7^*$	$8.3e7^*$	$8.3e7^*$	$8.3e7^*$	$5.1e7^*$	$5.1e7^*$	$5.1e7^*$	$5.1e7^*$
$S_q(0)$	0	0	0	0	0	0	0	0
$I_f(0)$	14	19	51	63	20	69	194	1000
$I_q(0)$	0^*	0^*	0^*	0^*	0^*	0^*	0^*	0^*
$I_j(0)$	114^*	114^*	114^*	114^*	87^*	87^*	87^*	87^*
$R(0)$	16^*	16^*	16^*	16^*	16^*	16^*	16^*	16^*
λ	0.022	0.022	0.019	0.035	0.09	0.004	0.01	0.99
α	0.046	0.047	0.031	$3.7e^{-10}$	0.11	0.026	0.04	1
μ	0^*	0^*	0^*	0^*	0^*	0^*	0^*	0^*
θ	1	1	0.5	0.38	1	0.92	0.5	0.26
γ	0.04	0.04	0.04	0.03	0.02	0.03	0.026	0.012
ν	614	19	40	–	4163	368	546	–
z	13	2	–	–	15	2	–	–
β	0.13	0.99	1	1	0.15	0.87	1	1

*Fixed parameters during parameter estimations

3.2.2 Vector-Borne Mosquitoes Transmission: Dengue Case

In this section, we present one model for indirect transmission (vector-borne diseases as seen in Fig. 6). We developed the compartmental model (9) following two criteria:

- The periodicity in which some countries report arboviral cases, i.e., one epidemiological week.
- The implementation of a discrete structure and both types of infection proposed probabilities. Because of the natural history of the disease, and in contrast to the COVID-19 case, $\widetilde{G}_{hm}(S_h, I_h, N_h)$ and $\widetilde{G}_{mh}(S_h, S_m, I_m)$ defined in (11)–(12) are the base probabilities to describe the human–mosquito and mosquito–human interactions, respectively. Thus, the analysis focused on the performance of both probabilities together.

The first criteria imply some reductions in expressions and the number of stages. The incubation periods are implicit in the period for the individuals to pass from susceptible to infected, e.g., if this week some individuals had an infectious interaction, then the next week they would enter the infected compartment. It matches the low limit of the intrinsic and extrinsic incubation periods reported in the literature, about 4–10 days and 8–12 days for dengue (World Heatlh Organization 2021), respectively.

The vector-borne model follows the same idea of compartment flux defined by event probabilities: the contact within two populations (humans and mosquitoes) produces the infectious individuals. In Table 3, we present the parameter definitions for the

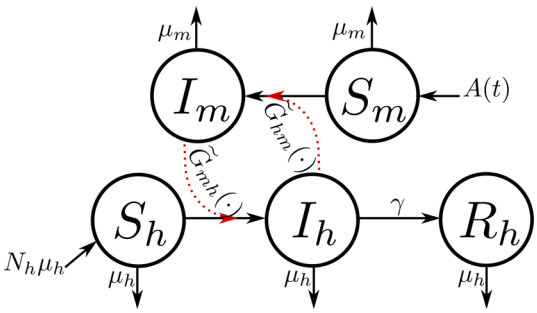

Fig. 6 Representation of the SIR vector-borne model that includes different compartments for human and vector populations (color figure online)

model.

$$\begin{aligned}
S_m(t+1) &= S_m(t)(1-\beta_{hm}\widetilde{G}_{hm}(\cdot))(1-\mu_m) + A(t)\\
I_m(t+1) &= S_m\beta_{hm}\widetilde{G}_{hm}(\cdot)(1-\mu_m) + I_m(t)(1-\mu_m)\\
S_h(t+1) &= S_h(t)(1-\beta_{mh}\widetilde{G}_{mh}(\cdot))(1-\mu_h) + N_h\mu_h\\
I_h(t+1) &= S_h(t)\beta_{mh}\widetilde{G}_{mh}(\cdot)(1-\mu_h) + I_h(t)(1-\gamma)(1-\mu_h)\\
R_h(t+1) &= R_h(t)(1-\mu_h) + I_h(t)(1-\mu_h)\gamma
\end{aligned} \tag{9}$$

As we mentioned in Sect. 2.4, we disaggregate a model estate (I_h) to fit it to real data. The new output is the instantaneous infectious population because there is no actual cases information as the COVID-19 case as shown in:

$$I_{h_{ins}}(t+1) = S_h(t)\beta_{mh}\widetilde{G}_{mh}(\cdot)(1-\mu_h) \tag{10}$$

We implemented a recruitment expression to simulate the vector emerging dynamic for the aquatic population input. Note that the vector population is not constant and could vary over time according to the mortality and birth rate, which we defined as a discrete Ricker expression. The expression depends on the number of mosquitoes from two weeks ago, simulating the aquatic phase delay:

$$A(t) = rN_m(t-2)\exp\left(1-\frac{N_m(t)}{C_m}\right), \text{ with } N_m = S_m + I_m.$$

We implemented both contagion probabilities to describe two different infectious interactions, i.e., human to mosquito and mosquito to human. Also, we include the $\aleph$ expressions to model the heterogeneous mixing between humans and vectors. This approach represents another paradigm of infectious source interaction that we describe in Sect. 3.1.1.

- The function $\widetilde{G}_{hm}(S_h,\ I_h)$ is the human interaction probability, i.e, the probability of a susceptible mosquito to bite a infected human.

$$\widetilde{G}_{hm}(S_h,\ I_h,\ N_h) = 1-\left(1-\left[\frac{I_h(t)}{N_h(t)}\right]^{\aleph_h(S_h,\ I_h)}\right)^z \tag{11}$$

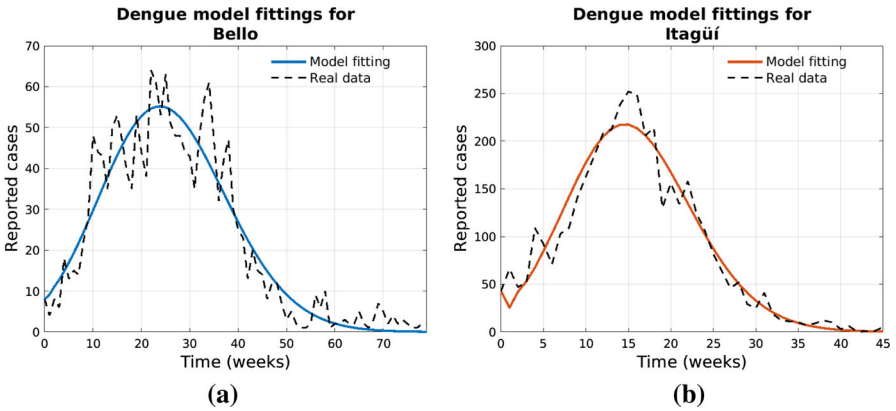

Fig. 7 Discrete model (9) fitted to real data of two endemic localities: **a** Bello (cost function 59) and **b** Itagüí (cost function 120) with the parameters presented in Table 3 (color figure online)

with $\aleph_h(S_h,\ I_h) = 1 + \frac{\nu_h I_h}{I_h + S_h}$ the connectivity expression related to the human population, $N_h = S_h + I_h + R_h$.

- The function $\widetilde{G}_{mh}(S_h,\ S_m,\ I_m)$ is the mosquitoes interaction probability, i.e., the probability of a susceptible human to be bitten by an infected mosquito:

$$\widetilde{G}_{mh}(S_h,\ S_m,\ I_m) = 1 - \left[1 - \frac{1}{S_h}\right]^{z I_m (S_h/N_h)^{\aleph_h(S_m,\ I_m)}} \tag{12}$$

with $\aleph_m(S_m,\ I_m) = 1 + \frac{\nu_m I_m}{I_m + S_m}$ the connectivity expression related to mosquitoes population.

We performed 2000 parameter estimations for the municipalities of Bello and Itagüí in Colombia using the model given in (9) and selected the best parameter estimations by its cost function value. Figure 7 presents the fits for each locality, in which the model fits the classical bell shape for the date related to dengue outbreaks.

In Table 3, we show the parameter values for the Bello and Itagüí model fits. We highlight that both localities are geographically close, and both outbreaks occurred at a similar time. We can identify parameters related to mosquitoes behavior and life cycle that are similar for both localities, e.g., the μ_m, z, r and C. On the other hand, the parameters β_{mh} and ν_m considerably vary between populations. Finally, note that ν_m and ν_h values are different for each locality are considerably low.

4 Discussion

Mathematical models are tools that represent relationships between the different components of a real system, such as disease transmission. Also, there are different ways to represent the systems through models, and their structure will depend on the researcher's vision and interpretation of the world. Even so, a disadvantage of

Table 3 Parameter and states (factors) definition for vector model

Factor	Definitions	Ranges	Bello	Itagüí
S_m	Susceptible mosquitoes	$[1e^4, 5e^5]$	28030	5550
I_m	Infected mosquitoes	[0,100]	4	4
S_h	Susceptible humans	–	$4.5e^{5}$*	$2.8e^{5}$*
I_h	Infected humans	–	8*	43*
R_h	Recovered humans	–	0*	0*
μ_h	Human probability of dying	–	0*	0*
μ_m	Mosquitoes probability of dying	[0,0.4]	0.35	0.4
γ	Recovered probability	[0.1,1]	1	0.4
z	Number of effective interactions	[1,10]	8	8
β_{hm}	Human-to-mosquito infection probability	[0,1]	0.87	0.94
β_{mh}	Mosquito-to-human infection probability	[0,1]	0.28	0.95
r	Mosquitoes reproductive rate	[0,60]	0.12	0.1
C	Mosquitoes carrying capacity	$[1e^3, 3.5e^4]$	325590	348490
ν_h	Human connectivity index	$[0, 1e^4]$	0.0006	0.0002
ν_m	Mosquitoes connectivity index	$[0, 3e^4]$	0.8	0.07

We present the range for each factor as the values that can take in initial conditions (states) and alongside its dynamics (parameters and functions). Also, estimated parameters for outbreaks occurred in Bello and Itagüí using the discrete model given in (9)
*Fixed parameters during parameter estimations

the traditional epidemiological models is the classical structures that model the contagion probabilities (Anastassopoulou et al. 2020; Catano-Lopez and Rojas-Diaz 2020). Thus, we developed theoretical functions based on the behavior of disease transmission in a contagion network that considers different factors associated with transmission dynamics, e.g., probabilities of establishing an infectious interaction, the number of infectious contacts and the level of connectivity or social distance within populations.

We could address the direct contagion probability for COVID-19 through four different expressions ($\widetilde{G}_1$, $\widetilde{G}_2$, $\widetilde{G}_3$, and $\widetilde{g}_3$). In contrast to dengue, in which the contagion representation is different because of the presence of two populations (human and vector populations with $\widetilde{G}_{hm}$ and $\widetilde{G}_{mh}$), the infection paradigm will depend on the definition of the disease interactions. Alternative probabilities described in the literature focused on different ways of representing contagion, e.g., for vector-borne disease with heterogeneous populations (Kong et al. 2018), the contagion probability in terms of distance between people in COVID-19 (Cabrera et al. 2021), among others. Those expressions sometimes have a numerous parameters to estimate or measure in the field (Zhou et al. 2004; Cabrera et al. 2021; Liu et al. 2021).

We developed probability functions that improve modeling diverse infectious behaviors, i.e., generating plateau or oscillation patterns for discrete-time model simulation or fitting. These dynamics match some endemicity triggered by social issues, e.g., the COVID-19 that is starting to deepen in some localities (Antia and Halloran 2021). Even so, other diseases show sporadic outbreaks triggered by environmental

conditions after remaining endemic (d'Onofrio and Manfredi 2009; Cruz-Pacheco et al. 2009). Thus, with the emerging diseases in recent years, we might explore more complex expressions for describing their infection dynamics. Following the idea proposed by (Cabrera et al. 2021), the infection behavior is a nonlinear process; thus, the probability of infection should be treated in this way. For example, as the number of infected increases, the probability of becoming infected may decrease because of burnout of the contagion networks as by the action of public policies. With the expression $\aleph$, we provide a dynamic similar to that described through the idea of infection networks, and we can identify that the third condition, described in Sect. 2.3, is not mandatory for all diseases.

We focused on avoiding complexity in parameters and their definition; they are immediately interpretable in dimensional units and biological sense. The parameters could vary through localities and diseases, in which it is possible to identify different epidemiological behaviors. To evaluate the proposed probabilities, we perform the parameter estimation for different localities and diseases because we focus both expressions on the contagion interaction performed by the susceptible or the infected population. In the COVID-19 case, we can implement all probabilities proposed depending on the modeler interest and model approach because of the behavior of the diseases, in which the paradigm for this infectious disease can be abroad from infected searching interactions over susceptible and vice versa. On the other hand, for vector-borne diseases, the general contagion process should be a mix of the proposed probabilities because of the biological interpretation of the mosquitoes feeding, i.e., $\widetilde{G}_{hm}$ for the mosquito-to-human infection and $\widetilde{G}_{mh}$ for the human-to-mosquito infection.

With the COVID-19 case, we selected two countries that differed on social behavior, disease control and population density (Jang et al. 2021). We compare, for both localities, the approach of the proposed expressions and classical probabilities. First, we noted that the parameter ν causes the model to fit two consecutive disease oscillations in the cases of classical and proposed contagion expressions. In some cases, consecutive oscillations could be generated by changes in control policies, the increase of the connection of individuals inside the population, or other external changes (d'Onofrio and Manfredi 2009). We can see these variations through the connectivity parameter ν using our proposed expressions. Then, comparing the parameters obtained for South Korea and Germany for $\widetilde{G}_1$, $\widetilde{G}_2$ and $\widetilde{G}_3$; we can see that both localities share similar quarantine and identification parameters. We highlight the values obtained for ν, which are considerably different for south Korea and Germany in the three scenarios, that indicate the first locality is less connected than the second one.

In the specific case of South Korea, the country had a less stringent containment policy than countries such as Germany (Jang et al. 2021) but had a greater level of contact tracing because of their previous experience with a large MERS coronavirus outbreak (Nouvellet et al. 2021; Lim et al. 2021). Thus, South Korea had a greater ν value than Germany because of their efficient policies. With these cases, we highlight that the ν parameter could describe the connectivity of a locality through its density, where a high-density population could present a low ν and vice versa. Also, a high ν parameter could represent social characteristics in localities with high density, i.e., a high value of ν in a population with high density describes the potential of lockdown,

restrict the connectivity between its inhabitants, or a high capability of tracing infection networks.

In the dengue case, we selected two localities geographically close to each other: Bello and Itagüí in Colombia. These localities presented similar values of infectious interactions (8 per week) that could result from the host-seeking behavior of the mosquitoes that can bite on multiple occasions until fill up (Farjana and Tuno 2013). Bello had lower values of β_{hm} and β_{mh} that could show a fewer infection potential linked to mosquito intrinsic or extrinsic conditions or dengue strain presented in this locality (Velasco et al. 2021). Note that for the ν parameter, both localities present lower values (compared to COVID-19) case, showing that mosquito and human populations are quite homogeneous for both localities. It could result from the disease and localities of study, i.e., other extrinsic conditions could affect the increase of the dengue outbreaks more than the mixing the individual populations. In contrast to the COVID-19, dengue outbreaks are related to the increase in mosquito populations and present successive outbreaks according to the climatic conditions as the *El Niño–Southern Oscillation* (Vincenti-Gonzalez et al. 2018).

The model fits the outbreaks we introduced in this study for the dengue case in two different study zones. Thus, we highlight for future works to consider climatic conditions even to model endemic and oscillatory behaviors alongside contagion probabilities. Also, we can implement discrete models alongside the proposed probabilities to develop control policies for different diseases, e.g., controlling the disease propagation by reducing the number of infectious interactions or the connectivity among the population. Decision-makers could implement these developments using mathematical models for different diseases and model paradigms.

5 Conclusions

We proposed contagion probability functions based on the behavior of disease transmission in a contagion network. We incorporated the notion of population heterogeneity through the concept of exhaustion of local contagions in the network with interpretable parameters at the biological level. These functions obey two paradigms of contagion: when the infected perform the interaction over the susceptible and vice versa. We took COVID-19 and dengue as case studies for both contagion approaches. It was possible to fit a discrete model to the dynamics of dengue and COVID-19 cases. The last one fits the oscillations in the infectious data for the localities of Germany and South Korea. Also, future investigation in control development would include the ν and z parameters to provide relevant information for developing public policies based on mathematical models, e.g., simulating it as a social distancing process or the heterogeneity level of the populations.

Acknowledgements This study was supported by *Universidad EAFIT*, Grant Number 954-000002. We thank Professor Henry Laniado Rodas for several helpful discussions.

Declarations

Conflict of interest The authors declare that they have no known competing financial interests or personal relationships that could have appeared to influence the work reported in this paper.

Appendix A Probabilities in the Literature

see Table 4.

Table 4 Structures implemented in mathematical models to describe contagion interactions. Some of these expressions share parameters as β the infection rate, for vector-borne diseases, a is the average biting rate, N_h for total host populations, I_v for infected vector

Structure	Parameters	Model type	Ref.
$\beta F\,(1 - P_r/(P_r + Z))$	F: free vector P_r: susceptible and infected host Z: vector searching	Continuous SIRD vector for black death	(Monecke et al. 2009)
$\beta I/N$	–	Continuous SIRD for COVID-19	(Sen and Sen 2021)
$k \ln(1 + \alpha p_v I_v/(kN_h))$	k: Gamma distribution with shape parameter p_v:Transmission probability from vector to human per bite a: number of bites	Continuous SEIRD vector for dengue	(Kong et al. 2018)
$a\beta I_v/N_h$	–	Discrete and continuous SIRD vector for West Nile virus and dengue	(Wonham et al. 2004) (Li and Li 2018)
$\beta\left[2\bar{D}_*/(\bar{D}_* + D)\right]^{\nu}$	D: interaction distance $D*$: natural equilibrium $D'*$: scaling distance ν: decrease in the infectious rate with distance	Continuous SIR for COVID-19	(Cabrera et al. 2021)
$b(\alpha P+\alpha A+I)/N$	α: transmission rate of unreported cases P: reported infectious A: isolation in hospital	Continuous SAPHIRE for COVID-19	(Purkayastha et al. 2021)

Table 4 continued

Structure	Parameters	Model type	Ref.
$(1-\rho)\beta(I+\epsilon E+A)$	ϵ: Infection rate in incubation period ρ: Probability of susceptibility to isolation	Continuous SEIRD for COVID-19	(Liu et al. 2021)
$I\beta/(1+\beta_M M)$	β_M : the efficacy of the awareness programs M: monotonic decreasing function of the number of campaigns	Continuous SIR for HIV/AIDS	(Greenhalgh et al. 2015)
$(\beta I/(1+\alpha I)$	α: The reciprocal of half-saturation	Continuous SIRV	(Masoumnezhad et al. 2020)
$\lambda_a[1-(1-\gamma_1)(1-\gamma_2)]+(1-\lambda_a)\gamma_2$	λ_a: proportion of one-year-old females γ_1 and γ_2: exposure probabilities during the lambing and the milking	Discrete SEIR for scrapie lambs	(Sabatier et al. 2004)
(31 + t)/(22 + 5t)	t: time	Discrete SEIR-QJ	(Zhou et al. 2004)

Appendix B Mathematical Properties of Contagion Probability Functions

In this section, we present the mathematical properties for the new contagion probabilities described above, following the criterion described in Sect. 2.3. First, note that the expression $G(S,\ I,\ N)$ exhibits the three conditions required for the infection function since they hold fixed values of S and $0 \leq I/M \leq 1$ in $g_1(S,\ I,\ N)$ and $g_2(I,\ N)$, so $G(S,\ I,\ N) \longrightarrow g_1(S,\ I,\ N)$ as long as $I/M \longrightarrow 0$, and we can state that effect of $g_2(I,\ N)$ is insignificant whether the number of I remains proportionally low.

Now, we will focus on the asymptotic of $g_1(S,\ I,\ N)$ and $g_2(I,\ N)$, where the expression zIS/N is a superior bound for the number of S that become exposed the disease ($Sg_1(S,\ I,\ N)$ and $Sg_2(I,\ N)$). Also, as the number of S is larger than the number of non-susceptible, i.e., $S/N \rightarrow 1$, then the number of individuals from S that have contagious interactions approaches to the number of infectious interactions. We proof that (i) $g_1(S,\ I,\ N)S \leq zIS/N$, as long as $zIS/N \geq 1$, and (ii) $1 > Sg_1(S,\ I,\ N)$ for the case of $0 < zIS/N < 1$.

Theorem 1 *If* $g_1(S,\ I,\ N) = 1 - \left[1 - \frac{1}{S}\right]^{\frac{zIS}{N}}$

1. *and* $\frac{zIS}{N} \geq 1$ *then* $Sg_1(S,\ I,\ N) \leq \frac{zIS}{N}$
2. *and* $0 < zI\frac{S}{N} < 1$ *then* $Sg_1(S,\ I,\ N) < 1$

Proof To prove 1 consider $x = -1/S$ and $\tau = \frac{zIS}{N}$, with $S \geq 1$ for all t. It is clear that $x \geq -1$. Then, by applying the Bernoulli's inequality[1] the conclusion follows.

To prove 2, given that $S \geq 1$, under $0 \leq 1 - \frac{1}{S}$ and $0 < \tau < 1$ we have that $1 - 1/S < [1 - 1/S]^{\tau}$. Then

$$1 - \left[1 - \frac{1}{S}\right]^{\tau} < \frac{1}{S} \text{ and } Sg_1(S,\ I,\ N) < 1.$$

□

Demonstration for superior bound of $g_2(I,\ N)$ is analogous. The proof of the second condition given in Sect. 2.3 for g_1 and g_2 is followed by considering $\frac{I}{N} = 0$.

Finally, checking the third property, we derivative each probability in terms of $x = I/N$. For $g_1(S,\ I,\ N)$ we have:

$$\frac{\partial g_1(x,\ N)}{\partial x} = -S\, z\, \log(1 - 1/S)\ (1 - 1/S)^{S\,x\,z}$$
$$\frac{\partial^2 g_1(x,\ N)}{\partial x^2} = -S^2\, z^2 \log(1 - 1/S)^2\ (1 - 1/S)^{S\,x\,z}$$

$\frac{\partial g_1(x,\ N)}{\partial x} \geq 0$ since $z \geq 0$, and $\frac{\partial^2 g_1(x,\ N)}{\partial x} < 0$ since $S > 1$ and $x \neq 0$. For $g_2(I,\ N)$

$$\frac{\partial g_2(x,\ N)}{\partial x} = z\,(1 - x)^{z-1}$$
$$\frac{\partial^2 g_2(x,\ N)}{\partial x^2} = -z\,(1 - x)^{z-2}\,(z - 1)$$

Note that all expression meet $0 \leq x \leq 1$.

Thus, $\frac{\partial g_2(x,\ N)}{\partial x} > 0$ and $\frac{\partial^2 g_2(x,\ N)}{\partial x} < 0$.

References

Allen LJ (1994) Some discrete-time SI, SIR, and SIS epidemic models. Math Biosci 124(1):83–105. https://doi.org/10.1016/0025-5564(94)90025-6

Anastassopoulou C, Russo L, Tsakris A et al (2020) Data-based analysis, modelling and forecasting of the COVID-19 outbreak. PLoS ONE 15(3):e0230405. https://doi.org/10.1371/journal.pone.0230405

Antia R, Halloran ME (2021) Transition to endemicity: understanding COVID-19. Immunity 54(10):2172–2176. https://doi.org/10.1016/j.immuni.2021.09.019

Cabrera M, Córdova-Lepe F, Gutiérrez-Jara JP et al (2021) An SIR-type epidemiological model that integrates social distancing as a dynamic law based on point prevalence and socio-behavioral factors. Sci Rep. https://doi.org/10.1038/s41598-021-89492-x

Cao H, Tan H (2015) The discrete tuberculosis transmission model with treatment of latently infected individuals. Adv Differ Equ. https://doi.org/10.1186/s13662-015-0505-8

Castillo-Chavez C, Yakubu AA (2001) Discrete-time s-i-s models with complex dynamics. Nonlinear Anal Theory Methods Appl 47(7):4753–4762. https://doi.org/10.1016/s0362-546x(01)00587-9

Catano-Lopez A, Rojas-Diaz D (2020) Modelos discretos de transmisión de COVID-19 y publicaciones preeliminares en la ciencia: una búsqueda sistematizada. https://doi.org/10.1590/scielopreprints.1076

[1] For all $x \in \mathbb{R}$ such that $x \geq -1$ and any real number $\tau \geq 1$, it is true that $(1 + x)^{\tau} \geq 1 + \tau x$.

Chávez JP, Götz T, Siegmund S et al (2017) An SIR-dengue transmission model with seasonal effects and impulsive control. Math Biosci 289:29–39. https://doi.org/10.1016/j.mbs.2017.04.005
Cruz-Pacheco G, Esteva L, Vargas C (2009) Seasonality and outbreaks in west Nile virus infection. Bull Math Biol 71(6):1378–1393. https://doi.org/10.1007/s11538-009-9406-x
DANE (2011) Departamento Administrativo Nacional de Estadística: Boletín: Censo General 2005. https://goo.gl/JSWVRr
Dong E, Du H, Gardner L (2020) An interactive web-based dashboard to track COVID-19 in real time. Lancet Infect Dis 20(5):533–534. https://doi.org/10.1016/s1473-3099(20)30120-1
d'Onofrio A, Manfredi P (2009) Information-related changes in contact patterns may trigger oscillations in the endemic prevalence of infectious diseases. J Theor Biol 256(3):473–478. https://doi.org/10.1016/j.jtbi.2008.10.005
Farjana T, Tuno N (2013) Multiple blood feeding and host-seeking behavior in *Aedes aegypti* and *Aedes albopictus* (Diptera: Culicidae). J Med Entomol 50(4):838–846. https://doi.org/10.1603/me12146
Fink JB, Ehrmann S, Li J et al (2020) Reducing aerosol-related risk of transmission in the era of COVID-19: an interim guidance endorsed by the international society of aerosols in medicine. J Aerosol Med Pulm Drug Deliv. https://doi.org/10.1089/jamp.2020.1615
Greenhalgh D, Rana S, Samanta S et al (2015) Awareness programs control infectious disease: multiple delay induced mathematical model. Appl Math Comput 251:539–563. https://doi.org/10.1016/j.amc.2014.11.091
Hernandez-Ceron N, Feng Z, Castillo-Chavez C (2013) Discrete epidemic models with arbitrary stage distributions and applications to disease control. Bull Math Biol 75(10):1716–1746. https://doi.org/10.1007/s11538-013-9866-x
Jang SY, Hussain-Alkhateeb L, Ramirez TR et al (2021) Factors shaping the COVID-19 epidemic curve: a multi-country analysis. BMC Infect Dis. https://doi.org/10.1186/s12879-021-06714-3
Kong L, Wang J, Li Z et al (2018) Modeling the heterogeneity of dengue transmission in a city. Int J Environ Res Public Health 15(6):1128. https://doi.org/10.3390/ijerph15061128
Li Y, Li J (2018) Discrete-time model for malaria transmission with constant releases of sterile mosquitoes. J Biol Dyn 13(sup1):225–246. https://doi.org/10.1080/17513758.2018.1551580
Lim B, Hong EK, Mou J et al (2021) COVID-19 in Korea: success based on past failure. Asian Econ Pap 20(2):41–62. https://doi.org/10.1162/asep_a_00803
Liu XX, Fong SJ, Dey N et al (2021) A new SEAIRD pandemic prediction model with clinical and epidemiological data analysis on COVID-19 outbreak. Appl Intell 51(7):4162–4198. https://doi.org/10.1007/s10489-020-01938-3
Martcheva M (2015) An introduction to mathematical epidemiology. Springer, Berlin. https://doi.org/10.1007/978-1-4899-7612-3
Masoumnezhad M, Rajabi M, Chapnevis A et al (2020) An approach for the global stability of mathematical model of an infectious disease. Symmetry 12(11):1778. https://doi.org/10.3390/sym12111778
Monecke S, Monecke H, Monecke J (2009) Modelling the black death. A historical case study and implications for the epidemiology of bubonic plague. Int J Med Microbiol 299(8):582–593. https://doi.org/10.1016/j.ijmm.2009.05.003
Nouvellet P, Bhatia S, Cori A et al (2021) Reduction in mobility and COVID-19 transmission. Nat Commun. https://doi.org/10.1038/s41467-021-21358-2
Peña-García V, Triana-Chávez O, Mejía-Jaramillo A et al (2016) Infection rates by dengue virus in mosquitoes and the influence of temperature may be related to different endemicity patterns in three Colombian cities. Int J Environ Res Public Health 13(7):734. https://doi.org/10.3390/ijerph13070734
Purkayastha S, Bhattacharyya R, Bhaduri R et al (2021) A comparison of five epidemiological models for transmission of SARS-CoV-2 in india. BMC Infect Dis. https://doi.org/10.1186/s12879-021-06077-9
Rojas-Díaz, Daniel and Vélez-Sánchez, Carlos Mario (2019) drojasd/gsua-csb: Gsua-csb v1.0. https://zenodo.org/record/3383316
Sabatier P, Durand B, Dubois M et al (2004) Multiscale modelling of scrapie epidemiology. Ecol Model 180(2–3):233–252. https://doi.org/10.1016/j.ecolmodel.2004.05.012
Sen D, Sen D (2021) Use of a modified SIRD model to analyze COVID-19 data. Ind Eng Chem Res 60(11):4251–4260. https://doi.org/10.1021/acs.iecr.0c04754
Usme-Ciro JA, Mendez JA, Tenorio A et al (2008) Simultaneous circulation of genotypes I and III of dengue virus 3 in Colombia. Virol J 5(1):101. https://doi.org/10.1186/1743-422x-5-101
Vega M (2013) Informe Final del Evento Dengue, año 2012

Velasco H, Laniado H, Toro M et al (2021) Modeling the risk of infectious diseases transmitted by *Aedes aegypti* using survival and aging statistical analysis with a case study in Colombia. Mathematics 9(13):1488. https://doi.org/10.3390/math9131488

Vincenti-Gonzalez MF, Tami A, Lizarazo EF et al (2018) ENSO-driven climate variability promotes periodic major outbreaks of dengue in Venezuela. Sci Rep. https://doi.org/10.1038/s41598-018-24003-z

Wonham MJ, de Camino-Beck T, Lewis MA (2004) An epidemiological model for west Nile virus: invasion analysis and control applications. Proc R Soc Lond B 271(1538):501–507. https://doi.org/10.1098/rspb.2003.2608

World Heatlh Organization (2021) Dengue and severe dengue. accessed: 2021 - may -30. https://www.who.int/news-room/fact-sheets/detail/dengue-and-severe-dengue

Zhou Y, Ma Z, Brauer F (2004) A discrete epidemic model for SARS transmission and control in China. Math Comput Model 40(13):1491–1506. https://doi.org/10.1016/j.mcm.2005.01.007